Kinetic Modeling of the Molecular Architecture of Cross-Linked Copolymers Synthesized by Controlled Radical Polymerization Techniques

Miguel AD. Gonçalves,[1] *Ivone MR. Trigo,*[1] *Rolando CS. Dias,**[1]
Mário Rui PFN. Costa[2]

Summary: A recently developed general kinetic approach, based on population balances in terms of generating functions, is applied to the modeling of the molecular architecture of branched copolymers produced through controlled radical polymerization (CRP) techniques, namely nitroxide-mediated radical polymerization (NMRP) and atom-transfer radical polymerization (ATRP). Thanks to this method, it is possible to carry out dynamic predictions of distributions of molecular weights, sequence lengths and *z*-average mean square radius of gyration of the products, both before and after gelation (whenever it occurs) with consideration of complex kinetic schemes. The model chemical systems styrene + divinylbenzene (S/DVB) and methyl methacrylate + ethylene glycol dimethacrylate (MMA/EGDMA) are experimentally investigated in order to assess the prediction capabilities of the aforementioned approach. Measurements of absolute molecular weights and *z*-average radius of gyration of the copolymers are performed for different times of polymerization using a SEC system with a refractive index detector coupled with MALLS. It is shown that the proposed computational tool can enhance the possibility of better design of these complex materials but additional studies concerning the impact of intramolecular cyclizations on the structure of materials synthesized at diluted conditions are needed.

Keywords: branching; crosslinking; kinetics; living polymerization; modeling

Introduction

In the last decade some works have explored the use of controlled radical polymerization techniques (CRP) to produce microgels (high molecular weight soluble polymers) and gels (insoluble networks) with improved homogeneity compared to those obtained by conventional free radical polymerization (FRP). Indeed, due to slow initiation and fast chain propagation with intermolecular termination reactions becoming highly hindered by spatial segregation, FRP leading to branched polymers or gels has a great tendency to produce inhomogeneous structures. [1]

The growing research activity in this domain is driven by the important applications of the produced materials in different application fields, namely in pharmaceutical and bioengineering industries or biomedicine. Better knowledge of the structural control offered by CRP is needed in order to be able to exploit this technique for obtaining useful products.

NMRP of vinyl/divinyl styrenic monomers using the stable radical TEMPO with the goal of avoiding the lack of structural

[1] LSRE-Instituto Politécnico de Bragança, Quinta de Santa Apolónia, 5300 Bragança, Portugal
Fax: (+351)273313051; E-mail: rdias@ipb.pt
[2] LSRE-Faculdade de Engenharia da Universidade do Porto, Rua Roberto Frias s/n, 4200-465 Porto, Portugal
Fax: (+351)225081666; E-mail: mrcosta@fe.up.pt

control characteristic of the FRP of the same monomers has been studied by several groups. [2–6]

Other recent works have reported the ATRP of methacrylates with divinyl monomers or the homopolymerization of the latter. [7–11] Several acrylate monomers and diacrylate cross-linkers have likewise been copolymerized by ATRP. [12,13] RAFT radical polymerization of oligo(oxyethylene) dimethacrylates with the purpose of making networks with beter homogeneity has also been recently described. [14]

In the present work, experimental and modeling studies for the NMRP of S/DVB and the ATRP of MMA/EGDMA are reported. For both systems, using different operational conditions (e.g. crosslinker amount), the dynamics of monomer conversion, molecular weights and z-average radius of gyration were experimentally measured in batch reactor through the analysis by SEC/RI/MALLS of polymer samples withdrawn at different polymerization times. It is shown that the general kinetic approach used in these modeling studies can be a valuable tool to design such materials.

Experimental Part

Experiments were carried out in a 2.5 dm^3 maximum capacity stainless steel semi-batch reactor of which a detailed description has already been presented elsewhere. [15] In this work the reactor was operated only in batch mode. In NMRP experiments, xylene of 98.5% purity, AIBN of 98% purity, TEMPO of 98% purity, styrene of 99% purity stabilized with 0.005% w/w 4-tert-butylcatechol and commercial grade divinylbenzene of 80% purity stabilized with 0.1% w/w 4-tert-butylcatechol were purchased from Sigma Aldrich and used as received. Commercial DVB is a mixture of isomers, 56.2% *m*-divinylbenzene and 24.2% *p*-divinylbenzene, plus 19.6% of ethylvinylbenzene. Xylene solvent is also a mixture of xylenes plus ethylbenzene ($\leq$ 25% in the latter component). In ATRP experiments, anisole of 99% purity, N,N-dimethylformamide (DMF) of 99.8% purity, MBPA (methyl α-bromophenylacetate) of 97% purity, HMTETA (1,1,4,7,10,10-hexamethyltriethylenetetramine) of 97% purity, Cu(I)Br of 98% purity, methyl methacrylate of 99% purity stabilized with 10 to 100 ppm monomethyl ether hydroquinone and ethylene glycol dimethacrylate of 98% purity stabilized with 100 ppm monomethyl ether hydroquinone were purchased from Sigma Aldrich and used as received.

Typically, NMRP and FRP S/DVB copolymerizations (see Table 1) were carried out as follows: the empty reactor was purged with an argon stream (40 cm^3/min) and the heating process to reach 130 °C was started. After 15 min, the desired quantities of styrene, xylene, divinylbenzene and TEMPO (in NMRP experiments) were charged to the reactor. Throughout the whole heating process the polymerization system was bubbled with the same argon flow rate of 40 cm^3/min. Owing to the heat losses, time delays between 100 and 120 min were needed to reach the set-point temperature of 130 °C in the FRP and NMRP experiments, respectively. This difference is explained by the heat generated by the auto-initiation of styrene in the conventional runs during the heating period. When the set-point was reached, samples of polymer were withdrawn from the reactor to be analyzed by SEC/RI/MALLS (details on this technique have been presented elsewhere [15]) and immediately afterwards AIBN was added to the system, defining the initial time $t = 0$ of the polymerization. The analysis of these samples confirmed the existence of thermal initiation of styrene during the heating process (monomer conversion of around 4% was experimentally measured) in conventional runs and also that this phenomena is negligible in the NMRP experiments. Later, samples of polymer were withdrawn from the reactor at pre-described polymerization times and analyzed by SEC/RI/MALLS. During the polymerization process the argon flow rate used to bubble the

Table 1.
Description of the set of experiments performed in the study of the TEMPO-mediated copolymerization of S/DVB at 130 °C.

Run	STY	DVB	AIBN	TEMPO	y_{DVB} (%)	TEMPO/AIBN
1	4.364	0.0	8.606×10^{-3}	0.0	0	0
2	4.351	2.157×10^{-2}	8.533×10^{-3}	0.0	0.5	0
3	4.364	0.0	8.649×10^{-3}	9.617×10^{-3}	0	1.1
4	4.350	2.211×10^{-2}	8.726×10^{-3}	9.607×10^{-3}	0.5	1.1
5	4.343	3.296×10^{-2}	8.540×10^{-3}	9.668×10^{-3}	0.75	1.1
6	4.331	5.360×10^{-2}	8.520×10^{-3}	9.534×10^{-3}	1.22	1.1
7	4.307	9.108×10^{-2}	8.457×10^{-3}	9.521×10^{-3}	2.07	1.1
8	4.247	18.744×10^{-2}	8.349×10^{-3}	9.377×10^{-3}	4.23	1.1
9	4.247	18.715×10^{-2}	8.352×10^{-3}	11.252×10^{-3}	4.23	1.3
10	4.247	18.693×10^{-2}	8.309×10^{-3}	16.874×10^{-3}	4.23	2.0

[a] Concentrations expressed in mol/dm^3.[b] Polymerizations in xylene solution with styrene/xylene = 1/1 (v/v).

system was reduced to 20 cm^3/min in order to decrease mass losses by evaporation. Note that the polymerization temperature is close to the xylene boiling point (around 140 °C) and that the reactor is operated at atmospheric pressure.

In ATRP experiments (see Table 2), MMA, EGDMA, solvent(s), CuBr and HMTETA were premixed at 60 °C for at least 30 min in a volumetric flask. Solubility problems with copper species in the polymerization system were avoided by using anisole [16] +DMF (even at a small amount) as a co-solvent. [17] That mixture was afterwards charged to the reactor, which had previously been purged with argon at a flow rate of 40 cm^3/min, and brought up to the desired temperature. This heating period is faster (at most 80 min) than with NMRP experiments because the operation temperature of ATRP runs was chosen in the range 60 to 90 °C. When the temperature set-point was attained, the bubbling process was maintained for one hour before initiation (as well as for the whole polymerization). Then, the initiator (MBPA) was added to the system defining $t = 0$. At pre-described polymerization times, samples of polymer were withdrawn from the reactor and analyzed by SEC/RI/MALLS.

Kinetic Modeling

Recently, a general kinetic approach allowing the prediction of molecular size distributions (MSD), sequence size distributions (SSD) and z-average radius of gyration (RG) was presented [18–21] based on work developed in the early nineties. [22] Indeed, it is possible to obtain the generating functions (GF) for the rate Equations for the formation of polymer species by chemical reactions ($G_{\mathcal{R}_P}$, $G_{\mathcal{R}_S}$

Table 2.
Description of the set of experiments performed in the study of the ATRP of MMA/EGDMA.

Run	T (°C)	MMA	EGDMA	MBPA	y_{EGDMA} (%)	DMF (%)
1	90	4.610	0.0	9.193×10^{-3}	0	2
2	80	4.656	0.0	9.337×10^{-3}	0	7
3	70	4.656	0.0	9.335×10^{-3}	0	7
4	90	4.545	2.304×10^{-2}	9.113×10^{-3}	0.5	4
5	80	4.635	2.360×10^{-2}	9.301×10^{-3}	0.5	7
6	70	4.635	2.356×10^{-2}	9.281×10^{-3}	0.5	7
7	90	4.555	1.153×10^{-2}	9.142×10^{-3}	0.25	4
8	90	4.558	0.843×10^{-2}	9.122×10^{-3}	0.18	4
9	90	4.561	0.470×10^{-2}	8.945×10^{-3}	0.1	4

Concentrations expressed in mol/dm^3.MBPA/CuBr/HMTETA = 1/1/1 in all Runs.Polymerizations in solution of Anisole + DMF with MMA/(Anisole + DMF) = 1/1 (v/v), % DMF is the volume fraction of DMF in the solvent.

and $G_{\mathcal{R}_{H_n}}$). The insertion of these GF in the population balance Equations (PBE) of a non-steady state perfectly mixed continuous stirred tank reactor (CSTR) yields PBE in terms of the GF of size distributions of mole concentrations of polymer degrees of polymerization, sequences and pendant chains, $G(s)$, $U(s)$ and $G_n^H(s^-, s^+)$, respectively:

$$\frac{\partial G}{\partial t} = G_{\mathcal{R}_P} + \frac{G_F(t) - G}{\tau} - \mathcal{R}_v G;$$
$$G_{|t=0} = G_0[\mathbf{s_0}(t, \mathbf{s})] \quad (1)$$

$$\frac{\partial U}{\partial t} = G_{\mathcal{R}_S} + \frac{U_F(t) - U}{\tau} - \mathcal{R}_v U;$$
$$U_{|t=0} = U_0[s_0(t, s)] \quad (2)$$

$$\frac{\partial G_n^H}{\partial t} = G_{\mathcal{R}_{H_n}} + \frac{G_n^H F(t) - G_n^H}{\tau} - \mathcal{R}_v G_n^H;$$
$$G_n^H|t = 0 = G_n^H 0\left[\mathbf{s_0^-}(t, \mathbf{s}^-), \mathbf{s_0^+}(t, \mathbf{s}^+)\right] \quad (3)$$

Eqs. (1)-(3) are non-linear first order partial differential Equations solvable by the method of the characteristics. Note that batch, plug flow and semi-batch reactors can be considered as special cases of a CSTR. Owing to their generality, master Equations Eqs. (1)-(3) can be applied in an automated way (as no analytical solution exists for most problems) to different polymerization systems and reactors involving branching (e.g. involving transfer to polymer and/or terminal branching [23,24]) and/or crosslinking of multivinyl monomers. These ideas have been recently applied to the modeling of FRP of MMA/EGDMA (batch reactor [25]) and S/DVB (in semi-batch reactor [15]).

This method is able to circumvent complexities of non-linear polymerizations (e.g. existence of multiple kinds of radicals and double bonds) and is free of several approximations of non-universal applicability (e.g. use of simplified statistical approaches, quasi-steady state for radical concentrations, closure conditions for the moments, absence of multiple radical centers in the same molecule, etc). A detailed discussion about the distinctive features of this approach relative to alternative methods can be found in the aforementioned works. [18–24]

Here, in NMRP S/DVB modeling studies, a kinetic scheme comprising a total of 36 chemical groups was considered as summarized in Table 3. Note that besides the 26 active groups presented in Table 3, an additional set of 10 inactive chemical groups (which react no further) were considered in the analysis of this polymerization system in order to have a detailed description of the molecular architecture of the products: polymerized monomer units (S, *m*-DVB and *p*-DVB), branching points (from *m*-PDB and *p*-PDB), polymerized fragments from initiator, dimer and solvent and saturated and head-head units (from termination reactions). It is important to note that since there are two isomers in commercial DVB, this polymerization system is more complex than analogue crosslinking processes using, for instance, pure diacrylates or dimethacrylates. It is known that *m*-DVB, *p*-DVB, *m*-PDB and *p*-PDB have different reactivities (see [15] and references therein) which have to be taken into account in the kinetic studies. Growing and dormant radicals arising from each kind of double bond were also distinguished because it is plausible that they also have different reactivities.

A set of 125 different chemical reactions was considered in the kinetic scheme of NMRP S/DVB, which are classified as follows:

- Mayo dimerization of styrene
- Thermal initiation of styrene
- Initiator decomposition
- Living/dormant exchange of radicals
- Initiation of monomers and pendant double bonds
- Propagation and termination
- Chain transfer to monomers, solvent, dimer and initiator

The large number of chemical reactions to be accounted for in this chemical system is a consequence of the number of different intermediate chemical species besides some important kinetic effects (e.g. thermal

Table 3.
Description of the active chemical groups considered in the modeling studies of the NMRP of S/DVB.

Group number	Group description	Alias
1	Styrene monomer (S)	M_1
2	*m*-Divinylbenzene monomer (*m*-DVB)	M_2
3	*p*-Divinylbenzene monomer (*p*-DVB)	M_3
4	Pendant double bond from *m*-DVB (*m*-PDB)	M_4
5	Pendant double bond from *p*-DVB (*p*-PDB)	M_5
6	Growing radical from S	R_1
7	Growing radical from *m*-DVB	R_2
8	Growing radical from *p*-DVB	R_3
9	Growing radical from *m*-PDB	R_4
10	Growing radical from *p*-PDB	R_5
11	Dormant radical from S	D_1
12	Dormant radical from *m*-DVB	D_2
13	Dormant radical from *p*-DVB	D_3
14	Dormant radical from *m*-PDB	D_4
15	Dormant radical from *p*-PDB	D_5
16	Initiator (AIBN)	I
17	Nitroxyl radical (TEMPO)	TEMPO
18	Radical from initiator (primary radical)	R
19	Dormant primary radical	SR
20	Radical from styrene (monomeric radical)	RM
21	Dormant monomeric radical	SM
22	Dimer of styrene	D
23	Radical from dimer	RD
24	Saturated nitroxyl radical	TS
25	Solvent	X
26	Radical from solvent	RX

initiation of styrene) caused by the relatively high temperature needed to carry out these polymerizations (130 °C).

A smaller set of chemical groups can describe the ATRP of MMA/EGDMA. Table 4 shows the 15 active species for that system. As in the previous example, besides the active groups, seven non-active groups have also been taken into account in order to obtain more detailed predictions about the molecular architecture of the products: polymerized MMA unit, polymerized EGDMA unit, crosslinking point, fragment of initiator, fragment of the solvent, saturated terminal unit (formed by termination by disproportionation), head-head unit (formed by termination by combination). This case study comprises 22 different

Table 4.
Description of the active chemical groups considered in the modeling studies of the ATRP of MMA/EGDMA.

Group number	Group description	Alias
1	MMA monomer	M_1
2	EGDMA monomer	M_2
3	Pendant double bond (PDB)	M_3
4	Growing radical from MMA	R_1
5	Growing radical from EGDMA	R_2
6	Growing radical from Pendant double bond	R_3
7	Dormant radical from MMA	D_1
8	Dormant radical from EGDMA	D_2
9	Dormant radical from Pendant double bond	D_3
10	Initiator (MBPA)	RX
11	Complex transition metal/ligand (CuBr/HMTETA)	C
12	Radical from initiator	R
13	Deactivator (cm^3/HMTETA)	CX
14	Solvent	S
15	Radical from solvent	RS

chemical species and a total count of 44 chemical reactions in the kinetic scheme, summarized as follows:

- Reversible activation/deactivation of initiator and radicals
- Initiation of monomers and pendant double bonds
- Propagation of monomers and pendant double bonds
- Chain transfer to monomers and solvent
- Termination by combination and disproportionation

Table 5 presents a basic set of rate coefficients considered in the modeling studies of the NMRP S/DVB. A similar set is presented in Table 6 for the ATRP MMA/EGDMA ($R = 8.314$ J mol^{-1}K^{-1} must be used in these Arrhenius equations). All these parameters have been collected from previous works (specified in Tables 5 and 6) concerning mostly the linear FRP and/or CRP of styrenic and methacrylate monomers. The extension to the non-linear case studies here considered is not straightforward because of the large number of kinetic parameters involved (note the number of radicals and double bonds with different reactivities) and little information can be found in the literature concerning the kinetics of the CRP of similar systems.[2,4] The calculations presented here are based on some postulated ratios of reactivity of the different kinds of radicals and double bonds which have been previously discussed in the framework of the FRP of S/DVB and MMA/EGDMA (see [15,25] and references therein). Nevertheless, it should be pointed out that the major parameters governing the crosslinking process are the reactivities of the pendant double bonds and these parameters will be estimated here using the available experimental data. These estimates have been obtained by neglecting intramolecular cyclizations. However, this can be an important issue even at 50% dilution, as it will be discussed below. Particularities of the activation/deactivation equilibrium in ATRP are also briefly addressed in the next section.

Results and Discussion

Comparison between measured and predicted monomer conversions for FRP and NMRP S/DVB copolymerizations are presented in Figure 1(a). Note that these simulations are almost insensitive to the reactivities of the pendant double bonds (the major factor influencing the crosslinking process) due to the low concentrations of these species in the reaction media.

Table 5.
Basic set of rate coefficients considered in the modeling studies of the NMRP of S/DVB.

Kinetic step	Rate coefficient expression	Ref.
Initiator thermal decomposition	$k_d = 4.31\times10^{15}\exp(-131.7\times10^3/RT)$ (s^{-1}) $f = 0.6$	[26]
Radicals deactivation	$k_{da} = 5.03\times10^{9}\exp(-15.57\times10^3/RT)$	[28–29]
Radicals activation	$k_a = 2\times10^{13}\exp(-124.2\times10^3/RT)$ (s^{-1})	[30,27,29]
STY propagation	$k_{p11} = 4.27\times10^{7}\exp(-32.5\times10^3/RT)$	[31]
Initiation of STY by primary radicals	$k_{iR1} = k_{iD1} = k_{iM1} = k_{iX1} = k_{p11}$	[32,29]
Chain transfer to monomer	$C_M = k_{fM11}/k_{p11} = 0.2198\exp(-23.5\times10^3/RT)$	[29,27,33]
Chain transfer to solvent	$k_{fX1} = 1.8$	[32]
Chain transfer to dimer	$k_{fD1} = 50$	[29,34]
Mayo dimerization of styrene	$k_{dim} = 188.97\exp(-67.7\times10^3/RT)$	[29]
Dimer decomposition	$k_{dim}^{-1} = 5.49\times10^{9}\exp(-106.1\times10^3/RT)$ (s^{-1})	[29,32]
Thermal initiation of styrene	$k_{iA} = 6.359\times10^{12}\exp(-153.1\times10^3/RT)$	[29]
Decomposition of dormant monomeric radicals	$k_{dec} = 5.7\times10^{14}\exp(-153.3\times10^3/RT)$ (s^{-1})	[29]
Rate enhancement reaction	$k_h = 10^{-3}$	[29]
Radical termination	$k_{p11}/\sqrt{k_t} = 426.4\exp(-26\times10^3/RT)$ $\alpha_{td} = k_{td11}/k_t = 0$, $\alpha_{tc} = k_{tc11}/k_t = 1$	[29,27,33] [26]

Kinetic parameters expressed in dm^{3}mol^{-1}s^{-1}, unless otherwise stated.

Table 6.
Basic set of rate coefficients considered in the modeling studies of the ATRP of MMA/EGDMA.

Kinetic step	Rate coefficient expression	Ref.
Initiator and radicals activation	$k_a = 140$ (EBPA at 22 °C in Acetonitrile)	[35]
	$k_a = 0.45$ (PS-Br at 110 °C in BPH)	[36,37]
Initiator and radicals deactivation	$k_{da} = 1.1\times10^7$	[36,37]
MMA propagation	$k_{p11} = 2.67\times10^6\exp(-22.36\times10^3/RT)$	[38]
Initiation of MMA by primary radicals	$k_{iR1} = 10k_{p11}$, $k_{iS1} = 10k_{p11}$	[37]
Chain transfer to monomer	$C_M = k_{fM11}/k_{p11} = 0.2\times10^{-4}$	[39]
Chain transfer to solvent	$C_S = k_{fS1}/k_{p11} = 0.2\times10^{-4}$	[39]
Radical termination	$k_{p11}/\sqrt{k_t} = 17.8\exp(-13.7\times10^3/RT)$	[40,26]
	$\alpha_{td} = k_{td11}/k_t = 0.6$, $\alpha_{tc} = k_{tc11}/k_t = 0.4$	

Kinetic parameters expressed in $dm^3mol^{-1}s^{-1}$, unless otherwise stated.

This means that with the basic set of kinetic parameters presented above it is possible to have a good description of the system in terms of polymerization rate. Predictions and experimental observations for $\overline{M}_n$ and $\overline{M}_w$ in FRP and NMRP linear runs ($y_{DVB} = 0$) are presented in Figure 1(b). A good agreement between experiments and theory is also observed. The ability of the present modeling studies to take into account the thermal initiation of styrene during the heating period (before introducing AIBN) is clear: simulations in Figure 1(b) show that self-polymerization of styrene during the heating process is negligible in NMRP (but not in FRP) due to the TEMPO stable radicals present in the polymerization system. This fact was experimentally confirmed in this work by measuring the monomer conversion before the addition of AIBN.

Figure 1(c) compares FRP and NMRP S/DVB runs with the same initial mole fractions of DVB ($y_{DVB} = 0.5\%$). These experiments and theoretical predictions confirm that NMRP can be used at least to have a better control on the dynamics of gelation of such polymerization systems. Figure 1(d) shows measured and predicted time evolutions of $\overline{M}_w$ in NMRP S/DVB runs with different mole fractions of crosslinker, stressing the influence of the initial amount of DVB in the dynamics of polymer properties. These experiments were simulated using the reactivity of PDBs as fitting parameters. It was estimated that PDBs present a lower reactivity as compared to styrene, with a ratio of propagation constants $r = k_p^*/k_{p11} = 0.35$. Other details concerning the postulated relation between the reactivity of other species with minor impact on the crosslinking process can be found elsewhere. [15] It is plausible that the reactivity ratios of PDBs here estimated are only apparent values due to the influence of intramolecular cyclization reactions which were neglected in these modeling studies. Intramolecular cyclizations should be more important at 50% dilution used in the present work as compared with bulk polymerizations used in related works [2] which have found an equal reactivity of PDB ($r = k_p^*/k_{p11} = 1$). An apparent decrease in the reactivity of PDB for diluted conditions has also been previously estimated by the same authors in the framework of FRP S/DVB. [15]

Figure 1(e) shows the measured and predicted time evolutions of the z-average radius of gyration ($\overline{R}_g$) of NMRP S/DVB samples synthesized with different initial amounts of DVB. A good agreement between measurements and simulations can be observed and it should be noticed that calculations of $\overline{R}_g$ have been carried out using the same set of kinetic parameters as in the calculations of molecular weights. The measurements of $\overline{R}_g$ were performed in THF solution using the MALLS system and our theoretical predictions of $\overline{R}_g$ are only valid for Gaussian chains [20] in a Θ solvent. To obtain the predictions presented here we have assumed equality of the expansion factors of branched and linear polymer

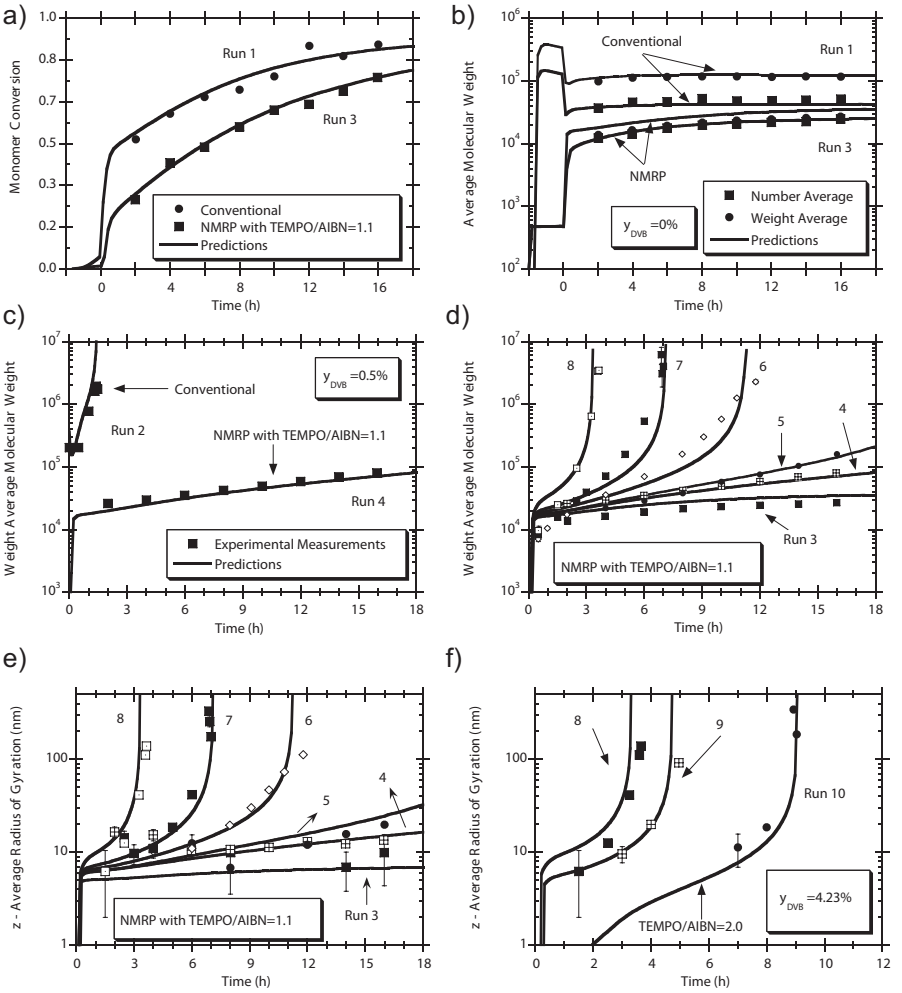

Figure 1.

(a) Predictions and experimental observations for monomer conversion in conventional and NMRP runs. Initial molar ratio TEMPO/AIBN = 1.1 in NMRP run. (b) Predictions and experimental observations for $\overline{M}_n$ and $\overline{M}_w$ in conventional and NMRP linear runs ($y_{DVB} = 0$). Initial molar ratio TEMPO/AIBN = 1.1 in NMRP run. Simulations include the thermal initiation of styrene during the heating period. (c) Measured and predicted time evolution of $\overline{M}_w$ in FRP and NMRP S/DVB runs with $y_{DVB} = 0.5\%$. (d) Measured and predicted time evolution of $\overline{M}_w$ in NMRP S/DVB runs with different amounts of crosslinker. Initial molar ratio TEMPO/AIBN = 1.1 in all runs. (e) Measured and predicted time evolution of $\overline{R}_g$ in NMRP S/DVB runs with different amounts of crosslinker. Initial molar ratio TEMPO/AIBN = 1.1 in all runs. (f) Comparison of experimentally observed and predicted influence of the initial molar ratio TEMPO/AIBN on the time evolution of $\overline{R}_g$ in NMRP S/DVB runs with a constant molar ratio of DVB ($y_{DVB} = 4.23\%$).

molecules, $\overline{R}_g/\overline{R}_{g,\theta} = 0.426\overline{M}_z^{0.1}$ (see [15] and references therein). The influence of the initial molar ratio of TEMPO/AIBN in the time evolution of $\overline{R}_g$ of S/DVB copolymers is presented in Figure 1(f). Again, despite the simplifications used in the computation of $\overline{R}_g$, a good agreement with measurements is observed. These results also show the possibility of using the ratio TEMPO/AIBN to control the dynamics of crosslinking of these products.

Figure 2(a) shows the measured dependencies of molecular weight (MW) on elution volume for NMRP synthesized

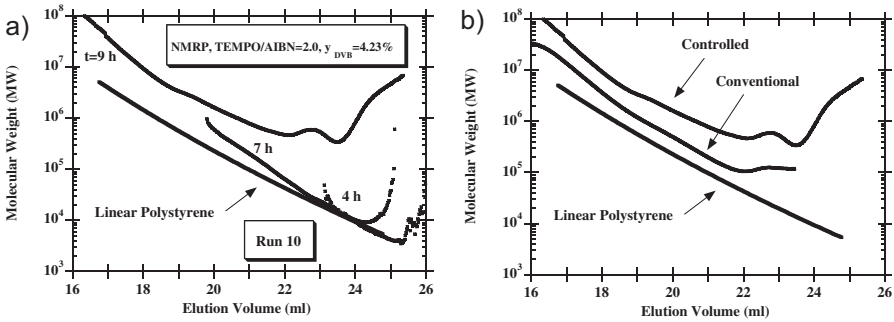

Figure 2.
(a) Observed relations of molecular weight vs. elution volume in SEC traces of NMRP synthesized samples of S/DVB corresponding to different polymerization times showing the gradual deviation from the linear case. (b) Observed relations molecular weight vs. elution volume in SEC traces of conventional and NMRP synthesized samples of S/DVB corresponding to polymerization times near the gel points. In both figures, molecular weight is that directly indicated by the software of the SEC/RI/MALLS system.

samples of S/DVB corresponding to different polymerization times. One can observe the progressive shift of the molecular architecture of the products from the linear case and an inversion in the relation of MW vs. elution volume (hydrodynamic radius) owing to the existence of polymer chains with the same molecular weight but different molecular sizes (elution volumes), as also observed for other non-linear polymerization systems. [41] Figure 2(b) confirms the presence of important differences in the molecular architecture of FRP and NMRP S/DVB samples collected near the corresponding gelation points. For the same molecular size (elution volume), NMRP products have higher molecular weight than the FRP materials. It can be concluded that NMRP is useful not only for manipulating the dynamics of crosslinking of these materials but also for modifying the structure of the products, with a likely impact on their end uses.

Figure 3(a) depicts a kinetic plot showing the living character of ATRP runs at different temperatures. It is well known that the variable $ln(M_0/M) = -ln(1-p)$ (where p is monomer conversion) should ideally follow a linear relation with polymerization time and this is confirmed by the experimental observations presented in Figure 3(a). The effects of ligand and initiator structures on the equilibrium constants for ATRP were recently studied [35] and for EBPA (ethyl α-bromophenylacetate) an activation rate constant $k_a = 140\ dm^3mol^{-1}s^{-1}$ is reported at 22 °C in acetonitrile and using the pair CuBr/HMTETA. In the same work, the correspondent equilibrium constant is estimated to be $K_{ATRP} = k_a/k_{da} = 1.1 \times 10^{-4}$. Similar rate coefficients should be valid for MBPA. Nevertheless, our kinetic measurements are consistent with much lower equilibrium constant values, namely of the order of 10^{-8}. A drop of polymerization rate in the presence of DMF is reported in the literature due to possible competitive complexation or ligand exchange of the copper species by DMF. [17] Other complexities related with the apparent external orders of the reactants, heterogeneity of the reaction medium or use of very reactive initiators can also contribute to modify the expected rate of polymerization. [37] Major deviations between measurements and predictions are also here observed at higher temperatures (90 °C), probably due to the increasing importance of side reactions and loss of the termination control characteristics of ATRP at high temperatures. Despite these descrepancies, once again, the reactivity of the PDB of EGDMA has an almost negligible impact on monomer conversion.

The predicted and experimentally observed influence of temperature on $\overline{M}_w$ in ATRP MMA/EGDMA with a constant

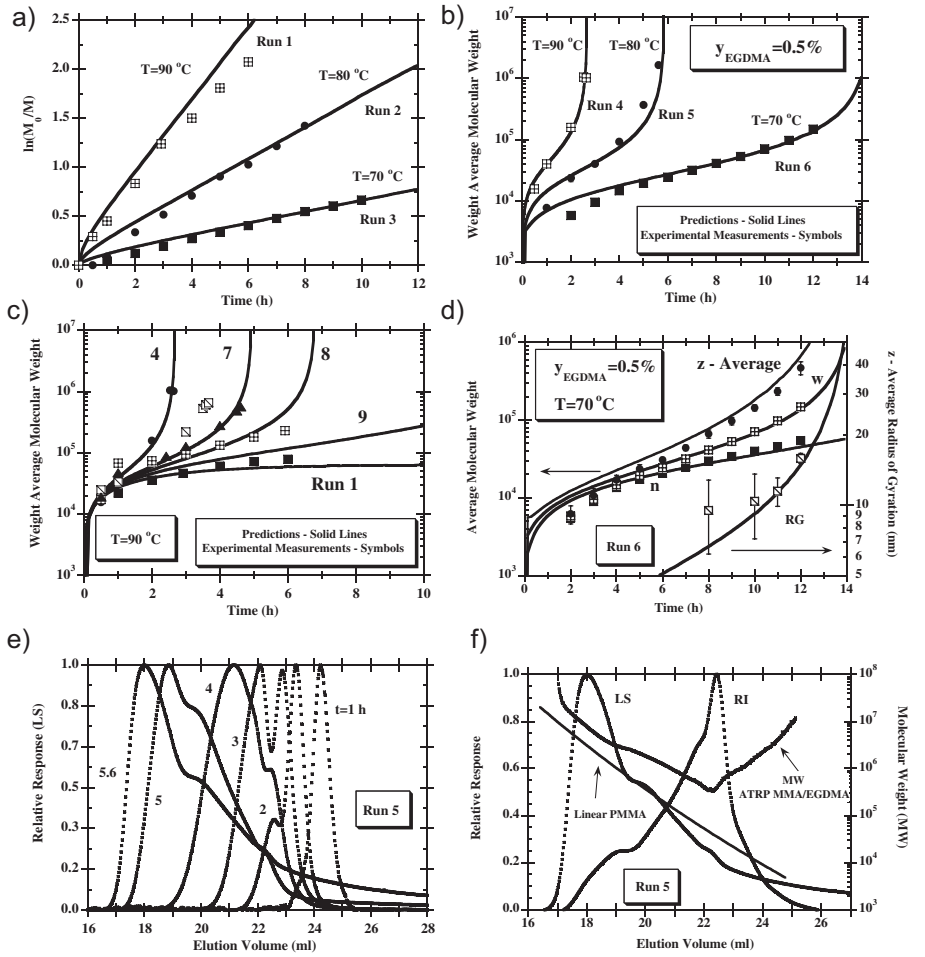

Figure 3.

(a) Predictions and experimental observations for monomer conversion in the ATRP of MMA/EGDMA at different temperatures. Initial molar ratio MBPA/CuBr/HMTETA = 1/1/1 in all runs. (b) Predicted and experimentally observed influence of the temperature on $\overline{M}_w$ in ATRP copolymerizations of MMA/EGDMA with constant initial mole fraction of crosslinker ($y_{EGDMA} = 0.5\%$). (c) Predicted and observed time evolution of $\overline{M}_w$ in copolymers produced by ATRP of MMA/EGMDA using different initial mole fractions of EGDMA at 90 °C. (d) Predicted and observed time evolution of $\overline{M}_n$, $\overline{M}_w$, $\overline{M}_z$ and $\overline{R}_g$ in the ATRP of MMA/EGMDA at 70 °C with $y_{EGDMA} = 0.5\%$. (e) Measured light scattering signal (90°) in the SEC traces of samples of MMA/EGDMA corresponding to different polymerization times showing the approach of the gel point ($T = 80$ °C, $y_{EGDMA} = 0.5\%$). (f) Molecular weight along the SEC trace for an ATRP synthesized sample of MMA/EGDMA with a polymerization time close to gel point.

mole fraction of crosslinker ($y_{EGDMA} = 0.5\%$) is presented in 9(b). These predictions were obtained using the reactivity of PDB of EGDMA which fits the experimental data. A reactivity ratio of PDB relative to the MMA double bonds $r = k_p^*/k_{p11} = 0.45$ was estimated. Nevertheless, as discussed above for NMRP S/DVB, probably the value of the reactivity ratio is underestimated due to the influence of intramolecular cyclizations which have been neglected in our calculations. For ATRP synthesized polyacrylate networks [12,13] equal reactivity of vinyl groups is reported ($r = 1$) as well as evidence for the increase of intramolecular cyclizations with

dilution. The effect of cyclization causing the underestimation of reactivity ratio of PDB was also identified in other works involving the FRP of dimethacrylates. [25] Figure 3(c) shows the predicted and observed time evolution of $\overline{M}_w$ in copolymers produced by ATRP MMA/EGDMA using different mole fractions of EGDMA at 90 °C. Here important deviations between measurements and predictions are observed at low EGDMA contents. This can be a consequence of the aforementioned lack of control of ATRP at high temperatures and of the major impact of intramolecular cyclizations at high monomer conversions (longer polymerization times).

Figure 3(d) shows predicted and observed time evolution of $\overline{M}_n$, $\overline{M}_w$, $\overline{M}_z$ and $\overline{R}_g$ in the ATRP of MMA/EGDMA at 70 °C with $y_{EGDMA} = 0.5\%$. A simultaneous good agreement between measurements and predictions of the average molecular weights and z-average radius of gyration is observed, confirming the good foundations of the present kinetic approach in the computation of some details of the molecular architecture of these complex materials. As in the NMRP of the S/DVB case study, the $\overline{R}_{g,\theta}$ predicted by our method was transposed to a good solvent (THF) assuming the equality of the expansion factors of branched and linear polymer molecules, $\overline{R}_g/\overline{R}_{g,\theta} = 0.438\overline{M}_z^{0.096}$ (see [25] and references therein for the MMA/EGDMA system).

Figure 3(e) shows the measured light scattering signal (90°) in the SEC traces of MMA/EGDMA samples corresponding to different polymerization times. Here the closeness to the gel point can be detected by the gradual formation of a cluster of high molecular weight albeit at very low concentration. Note that the IR signal corresponding to the high molecular weight region is very low, as depicted in Figure 3(f). In this figure it is also shown the molecular weight along the SEC trace for an ATRP synthesized sample of MMA/EGDMA corresponding to a polymerization time close to the gel point. Note that a huge deviation from the linear case is here identified, as also observed in the NMRP S/DVB samples. Figure 3(f) also shows that erroneous interpretations of chromatograms of non-linear polymers will result from using molecular weight calibration with linear polymers.

Conclusion

It has been shown that important features of the molecular architecture of the NMRP of S/DVB and the ATRP of MMA/EGDMA synthesized copolymers (in a 2.5 dm^3 reactor) can be measured using a SEC/MALLS system. Molecular architecture of both kinds of non-linear copolymers presents important differences not only as compared with the linear polymers but also with respect to the FRP of the same monomers.

A general kinetic approach allowing the prediction of the formation and final structure of these complex materials (such as average radii of gyration in sol), despite the large number of chemical groups and reactions involved, was applied to the modeling of these polymerization systems. This computational tool can enhance the possibilities of better design of the involved products and processes.

The influence of intramolecular reactions has been detected at 50% dilution, showing that at best only in bulk conditions [2] networks with small extent of cyclizations can be produced. The experimental results of this work agree with those reported for polyacrylate networks with ATRP [12,13] which have also provided evidence for intramolecular cyclizations at similar dilution ratios. Ongoing research is expected to provide more assertive results on this issue and start establishing the quantitative modeling of the effect of intramolecular reactions.

Acknowledgements: Financial support by Fundação para a Ciência e a Tecnologia (FCT), Ministry of Science and Technology of Portugal and the European Community through FEDER is gratefully acknowledged (projects POCI/

EQU/44784/2002 and POCI-PPCDT/EQU/60483/2004).

[1] A. Matsumoto, *Adv. Polym. Sci.* **1995**, *123*, 41.
[2] N. Ide, T. Fukuda, *Macromolecules* **1997**, *30*, 4268.
[3] S. Abrol, P. A. Kambouris, M. G. Looney, D. H. Solomon, *Macromol. Rapid Commun.* **1997**, *18*, 755.
[4] N. Ide, T. Fukuda, *Macromolecules* **1999**, *32*, 95.
[5] S. Abrol, M. J. Caulfield, G. G. Qiao, D. H. Solomon, *Polymer* **2001**, *42*, 5987.
[6] E. Tuinman, N. T. Mcmanus, M. Roa-Luna, E. Vivaldo-Lima, L. M. F. Lona, A. Penlidis, *J. Macromol. Sci.* **2006**, *43*, 995.
[7] Q. Yu, F. Zeng, S. Zhu, *Macromolecules* **2001**, *34*, 1612.
[8] A. R. Wang, S. Zhu, *Macromolecules* **2002**, *35*, 9926.
[9] A. R. Wang, S. Zhu, *Polym. Eng. Sci.* **2005**, *45*, 720.
[10] Q. Yu, J. Zhang, M. Cheng, S. Zhu, *Macromol. Chem. Phys.* **2006**, *207*, 287.
[11] Q. Yu, M. Zhou, Y. Ding, B. Jiang, S. Zhu, *Polymer* **2007**, *48*, 7058.
[12] H. Gao, K. Min, K. Matyjaszewski, *Macromolecules* **2007**, *40*, 7763.
[13] H. Gao, W. Li, K. Matyjaszewski, *Macromolecules* **2008**, *41*, 2335.
[14] Q. Yu, Y. Zhu, Y. Ding, S. Zhu, *Macromol. Chem. Phys.* **2008**, *209*, 551.
[15] M. A. D. Gonçalves, R. C. S. Dias, M. R. P. F. N. Costa, *Macromol. Symp.* **2007**, *259*, 124.
[16] J. Xia, K. Matyjaszewski, *Macromolecules* **1997**, *30*, 7697.
[17] S. Pascual, B. Coutin, M. Tardi, A. Polton, J.-P. Vairon, *Macromolecules* **1999**, *32*, 1432.
[18] M. R. P. F. N. Costa, R. C. S. Dias, *Chem. Eng. Sci.* **2005**, *60*, 423.
[19] R. C. S. Dias, M. R. P. F. N. Costa, *Polymer* **2006**, *47*, 6895.
[20] M. R. P. F. N. Costa, R. C. S. Dias, *Polymer* **2007**, *48*, 1785.
[21] R. C. S. Dias, M. R. P. F. N. Costa, *Macromol. React. Eng.* **2007**, *1*, 440.
[22] M. R. P. F. N. Costa, R. C. S. Dias, *Chem. Eng. Sci.* **1994**, *49*, 491.
[23] R. C. S. Dias, M. R. P. F. N. Costa, *Macromolecules* **2003**, *36*, 8853.
[24] R. C. S. Dias, M. R. P. F. N. Costa, *Macromol. Theory Simul.* **2005**, *14*, 243.
[25] I. M. R. Trigo, M. A. D. Gonçalves, R. C. S. Dias, M. R. P. F. N. Costa, *Macromol. Symp.* **2008**, *271*, 107.
[26] G. Moad, D. H. Solomon, *The Chemistry of Radical Polymerization* **2006**, 2nd Ed., Elsevier, Oxford.
[27] M. Zhang, W. H. Ray, *J. Appl. Polym. Sci.* **2002**, *86*, 1630.
[28] A. L. Beckwith, V. W. Bowry, K. H. Ingold, *J. Am. Chem. Soc.* **1992**, *114*, 4983.
[29] J. Belincanta-Ximenes, P. V. R. Mesa, L. M. F. Lona, E. Vivaldo-Lima, N. T. McManus, A. Penlidis, *Macromol. Theory Simul.* **2007**, *16*, 194.
[30] T. Fukuda, T. Terauchi, A. Goto, K. Ohno, Y. Tsujii, T. Miyamoto, S. Kobatake, B. Yamada, *Macromolecules* **1996**, *29*, 6393.
[31] M. Buback, R. G. Gilbert, R. A. Hutchinson, B. Klumperman, F.-D. Kuchta, B. G. Manders, K. F. O'Discoll, G. T. Russel, J. Schweer, *Macromol. Chem. Phys.* **1995**, *196*, 3267.
[32] Y. Fu, M. F. Cunningham, R. A. Hutchinson, *Macromol. React. Eng.* **2007**, *1*, 243.
[33] A. W. Hui, A. E. Hamielec, *J. Appl. Polym. Sci.* **1976**, *16*, 749.
[34] G. Greszra, K. Matyjaszewski, *Macromolecules* **1996**, *29*, 7661.
[35] W. Tang, Y. Kwak, W. Braunecker, N. V. Tsarevsky, M. L. Coote, K. Matyjaszewski, *J. Am. Chem. Soc* **2008**, *130*, 10702.
[36] K. Ohno, A. Goto, T. Fukuda, J. Xia, K. Matyjaszewski, *Macromolecules* **1998**, *31*, 2699.
[37] D. A. Shipp, K. Matyjaszewski, *Macromolecules* **2000**, *33*, 1553.
[38] S. Beuermann, M. Buback, T. P. Davis, R. G. Gilbert, R. A. Hutchinson, O. F. Olaj, G. T. Russel, J. Schweer, A. M. van Herk, *Macromol. Chem. Phys.* **1997**, *198*, 1545.
[39] R. A. Hutchinson, *Handbook of Polymer Reaction Engineering*, **2005**, Wiley-VCH.
[40] M. Fernández-Garcia, J. J. Martinez, E. L. Madruga, *Polymer* **1998**, *39*, 991.
[41] I. Bannister, N. C. Billingham, S. P. Armes, S. P. Rannard, P. Findlay, *Macromolecules* **2006**, *39*, 7483.

